Antiviral agent blocks breathing of the common cold virus

J. Kathleen Lewis*, Brian Bothner*, Thomas J. Smith†‡, and Gary Siuzdak*‡

*Departments of Molecular Biology and Chemistry, The Scripps Research Institute, La Jolla, CA 92037; and †Department of Biological Sciences, Purdue University, West Lafayette, IN 49707

ABSTRACT   A dynamic capsid is critical to the events that shape the viral life cycle; events such as cell attachment, cell entry, and nucleic acid release demand a highly mobile viral surface. Protein mass mapping of the common cold virus, human rhinovirus 14 (HRV14), revealed both viral structural dynamics and the inhibition of such dynamics with an antiviral agent, WIN 52084. Viral capsid digestion fragments resulting from proteolytic time-course experiments provided structural information in good agreement with the HRV14 three-dimensional crystal structure. As expected, initial digestion fragments included peptides from the capsid protein VP1. This observation was expected because VP1 is the most external viral protein. Initial digestion fragments also included peptides belonging to VP4, the most internal capsid protein. The mass spectral results together with x-ray crystallography data provide information consistent with a "breathing" model of the viral capsid. Whereas the crystal structure of HRV14 shows VP4 to be the most internal capsid protein, mass spectral results show VP4 fragments to be among the first digestion fragments observed. Taken together this information demonstrates that VP4 is transiently exposed to the viral surface via viral breathing. Comparative digests of HRV14 in the presence and absence of WIN 52084 revealed a dramatic inhibition of digestion. These results indicate that the binding of the antiviral agent not only causes local conformational changes in the drug binding pocket but actually stabilizes the entire viral capsid against enzymatic degradation. Viral capsid mass mapping provides a fast and sensitive method for probing viral structural dynamics as well as providing a means for investigating antiviral drug efficacy.

Human rhinovirus 14 (HRV14), the causative agent of the common cold, is a member of a family of animal viruses—the picornaviruses—whose other members include the polio, hepatitis A, and foot-and-mouth disease viruses (1). The HRV14 virion consists of an icosahedral protein shell, or viral capsid, surrounding an RNA core. The capsid is made up of 60 copies of each of four structural proteins, VP1–VP4. Based on crystal structure data (2), VP1, VP2, and VP3 compose the viral surface, whereas VP4 lies interior at the capsid/RNA interface. To examine the solution structure of HRV14, we used protein mass mapping, limited proteolysis with mass spectrometry (3, 4). Here the site-specific proteolytic degradation of a protein results in a set of digestion fragments which are subsequently mass analyzed by matrix-assisted laser desorption/ionization mass spectrometry (MALDI-MS). The resulting digestion fragments provide structural information concerning the individual capsid proteins as well as their protein–protein interactions, because available cleavage sites are dependent on both the tertiary and quaternary protein structure. For instance, cleavage sites residing on the exterior of the virus will be most accessible to the enzyme and therefore be among the first digestion fragments observed. Because proteolysis is performed in solution and can detect different conformational species, this method can contribute to an understanding of the dynamic domains within the virus structure.

MALDI-MS generates gas phase ions by the laser vaporization of a solid matrix/analyte mixture in which the matrix (usually a small crystalline organic compound) acts as a receptacle for energy deposition. MALDI-MS typically provides picomole sensitivity and accuracy on the order of 0.05% (i.e., ±0.5 Da on a 1,000-Da peptide). The relatively low number of charge states generated with MALDI (typically only the singly and doubly charged species are observed), along with its high sensitivity and ability to simultaneously generate ions from multicomponent mixtures, makes it especially well-suited for analyzing viral proteins and peptides resulting from proteolytic digests. In this study we demonstrate the use of MS to investigate the solution structural dynamics of HRV14 and the efficacy of the antiviral drug Win 52084.

MATERIALS AND METHODS

HRV14 was prepared as previously described (6) to a final concentration of 1 mg/ml in 10 mM TRIS buffer at pH 7.6. Trypsin digests were conducted at 25°C with 1 mg/ml virus in 25 mM Tris·HCl, pH 7.7. The enzyme to virus ratio (wt/wt) was adjusted to 1:100. Reaction volume was 10 μl, and 0.50 μl was removed from the reaction at each time (5, 10, and 60 min), placed directly on the MALDI analysis plate, and allowed to dry before the addition of matrix [0.5 μl of 3, 5-dimethoxy-4-hydroxy cinnamic acid (Aldrich) in a saturated solution of acetonitrile/water (50:50) 0.25% trifluoroacetic acid]. On-plate digestions (data not shown) were performed at room temperature by using a mass spectrometer sample plate derivatized with trypsin (Intrinsic Bioprobes, Tempe, AZ). MALDI-MS mass analysis was conducted by using a Perceptive Biosystems (Framingham, MA) Voyager Elite equipped with delayed extraction and a nitrogen laser. External mass calibration typically was accurate to 0.05% and allowed unequivocal assignment of most proteolytic fragments. The identity of trypsin released fragments was determined by the Protein Analysis Worksheet (PAWS, MacIntosh version 6.0b2, copyright 1995, Dr. Ronald Beavis) available on the Internet.

MALDI-MS mass analysis was conducted by using a Perceptive Biosystems Voyager Elite and a Kratos Analytical Instruments MALDI-IV, both equipped with delayed extraction and nitrogen lasers. All analyses were conducted by using 0.5 μl of 3,5-dimethoxy-4-hydroxy cinnamic acid (Aldrich) in a saturated solution of acetonitrile/water (50:50) 0.25% trifluoroacetic acid. External calibration typically was accurate to 0.05% and allowed unequivocal assignment of most proteolytic fragments.

Abbreviations: HRV14, human rhinovirus 14; MALDI, matrix-assisted laser desorption/ionization; FHV, Flock house virus; NIm, neutralizing immunogenic.
‡To whom reprint requests should be addressed. e-mail: tom@bragg.bio.purdue.edu and siuzdak@scripps.edu.

RESULTS AND DISCUSSION

Previous proteolytic time-course experiments on the Flock house virus (FHV) have clearly demonstrated (5), in combination with the x-ray data, that portions of the capsid proteins are transiently exposed on the viral surface. The time-course mass mapping of HRV14 performed in the present study revealed structural information in good agreement with the three-dimensional crystal structure (2) and, similarly to FHV, revealed results indicative of the transient exposure of internalized capsid proteins. Trypsin digests contained fragments resulting from the cleavage of residues residing near or included in the neutralizing immunogenic (NIm) sites (NIm-IA, NIm-IB, NIm-II, and NIm-III) (2) shown in Fig. 1 (*Inset*). Although the observation was expected, because NIm sites lie in loop regions on the exterior surface of the virus and are therefore easily accessible to proteases, such cleavages are significant evidence that mass mapping results are consistent with viral structure. Likewise, initial digestion fragments (fragments produced in the first 5 min of digestion) included sequences from the capsid protein VP1; this observation was expected because VP1 is considered the most external viral protein (2).

Also represented in the early stages of HRV14 digestions were fragments originating from VP4 (Fig. 1 and Table 1). This observation is particularly interesting in that VP4 is crystallographically defined as being internal to the larger capsid proteins (Fig. 1 *Inset*) and hence not expected to be readily accessible to proteolysis. When combined with the crystal structure data, the proteolysis results are consistent with a

Table 1. Trypsin fragments generated from HRV14 over the time course 1 h (as shown in fig. 1)

Time	Proteolytic fragments (viral protein)	*m/z* observed	*m/z* theoretical	% error
0	—	—	—	—
5	1–51 (VP4)	5562.8	5564.7	0.030
	9–62 (VP4)	5855.7	5855.4	0.005
	9–33 (VP4)	2831.3	2831.0	0.010
	1–8 (VP4)	1031.1	1030.9	0.020
	1–13 (VP1)	1430.4	1430.6	0.010
	31–94 (VP1)	6979.0	6977.8	0.020
10	13–52 (VP2)	4355.7	4355.8	0.002
	76–93 (VP3)	2012.2	2013.2	0.050
	27–54 (VP1)	3007.2	3007.4	0.006
	31–54 (VP1)	2513.1	2513.9	0.030
	55–73 (VP1)	2207.2	2207.4	0.009
	55–94 (VP1)	4483.7	4482.9	0.020
60	1–61 (VP3)	6688.1	6688.6	0.007
	40–61 (VP3)	2544.4	2545.0	0.020
	40–75 (VP3)	4145.0	4144.7	0.020
	144–174 (VP3)	3473.6	3475.0	0.040

dynamic or "breathing" capsid in which the different capsid proteins fluctuate between different conformations and specific protein regions can translocate to the capsid surface (Fig.
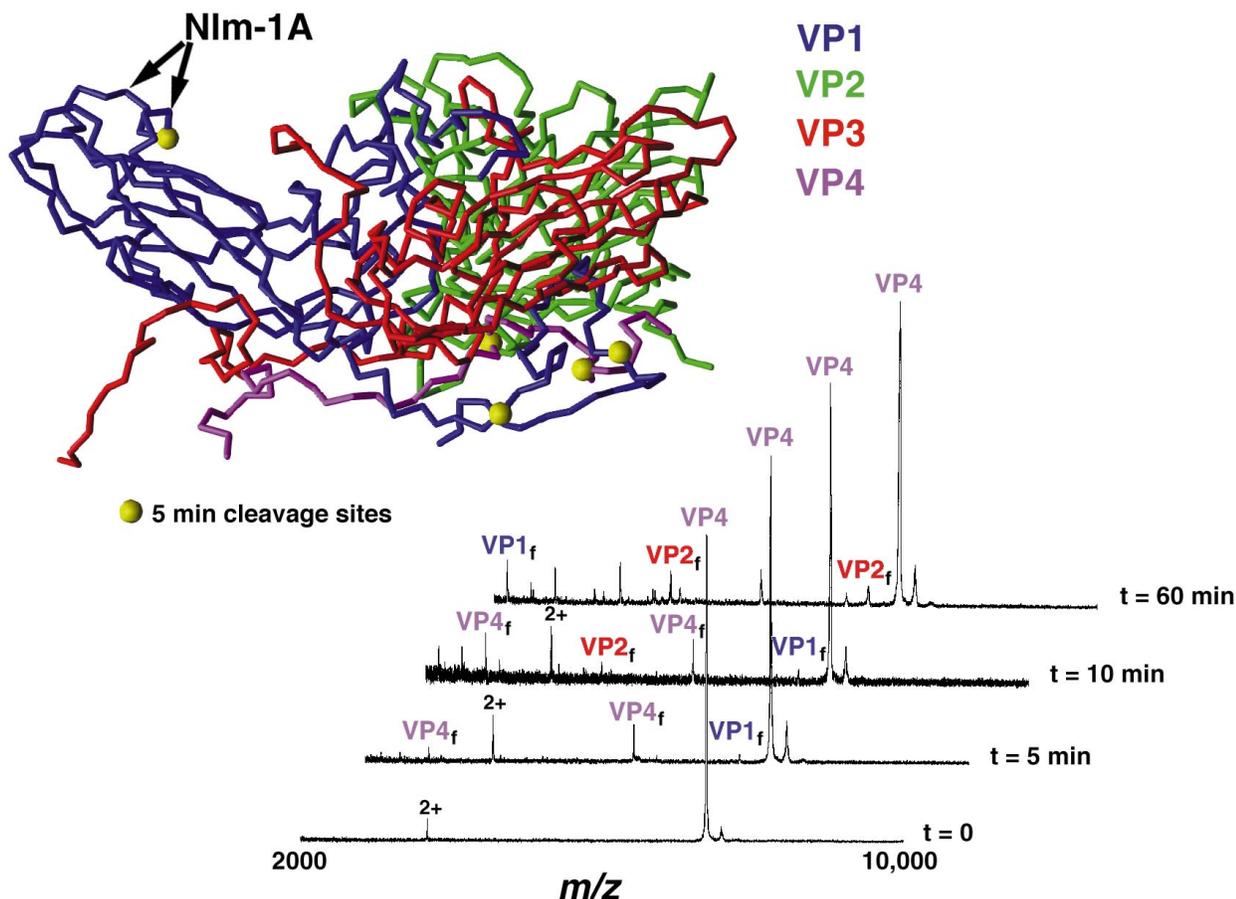

FIG. 1. Trypsin digestion time course of HRV14 (*Inset*). The asymmetric unit of HRV14 is shown such that the interior RNA is located at the bottom of the diagram, the nearest 5-fold axis on the left, and the nearest 2-fold axis on the right. VP1, VP2, VP3, and VP4 are blue, green, red, and mauve, respectively. Large yellow balls denote initial cleavage sites after a 5-min incubation with trypsin. Doubly charged species in the mass spectra are denoted by 2+. $T = 0$ represents undigested virus with VP4 observed at $m/z = 7{,}390.0$; VP1–VP3 (not shown) are observed at $m/z = 32{,}518.9$ (VP1 expected 32, 519.5 Da), 28,475.9 (VP2 expected 28, 477.4 Da), and 26,219.5 (VP3 expected 26, 217.8 Da).

2). A potential, although unlikely, explanation for the observation of digest fragments originating from VP4 is that a massive pore is exposed during the breathing process that allows trypsin to pass through. To test whether trypsin might enter the virion, digestions were performed with surface-bound enzymes. Whereas the digestion pattern changed when immobilized enzyme was used, buried residues and the NIm-IA site were still cleaved by the surface-bound enzyme. Therefore, a more likely explanation for the early observation of VP4 fragments can be derived from a thermodynamic model for HRV14 uncoating. In this model, HRV14 exists in at least two different structural states: one represented by the crystal structure where VP4 lies at the capsid/RNA interface, and the other, where VP4 protrudes from the viral interior and is accessible to proteases. Our results suggest that the energy barrier between these two states is relatively small because both are found at ambient temperatures. In addition, these results are similar to those from previous poliovirus studies, in which antibodies recognizing internal VP4 epitopes were found to bind when polio-virions were incubated with antibodies at physiological temperature (7). This was the first study to suggest that structural breathing (translocation of internal proteins to the exterior viral surface) may actually represent large dynamic changes in virion structure.

To determine the effects of drug binding on the viral capsid, enzymatic digestions were also performed in the presence of the antiviral agent WIN 52084. The x-ray crystal structure of HRV14 reveals a 25 Å deep canyon on the surface of the virion at each 5-fold axis of symmetry (8) that has been identified as the site of receptor attachment (9). WIN compounds bind to hydrophobic pockets in VP1, which lie beneath the canyon floor (10). Previous studies have shown that the binding of WIN compounds blocks cell attachment of some rhinovirus serotypes (11), inhibits the uncoating process, and stabilizes the viral capsid to thermal and acid inactivation (12–14). This stabilization occurs in spite of relatively minor changes in capsid structure (10). In the presence of the drug, digestion by the free and immobilized enzyme (data not shown) was significantly retarded by WIN 52084 after exposure to the enzyme for 3 h (Fig. 3), and even after 18 h, only two digestion

fragments were observed. Mass mapping of FHV in the presence of WIN 52084 revealed no inhibition of viral capsid degradation. Therefore, WIN inhibition of protease activity is clearly caused by specific effects on the availability of HRV14 cleavage sites and not on the protease itself (Fig. 4).

Our results, together with those of previous studies, suggest that drug binding not only affects local conformation in the drug pocket and canyon floor but has a global stabilizing effect on the entire viral capsid. Studies of a number of antiviral drugs against poliovirus have suggested that the drugs cause specific conformational changes in the viral capsid proteins (15). The authors hypothesized that at ambient temperatures the poliovirus samples a number of conformations and that the different drug compounds "locked" the capsid in one of these states. Our comparative digests suggest that this drug-induced stability significantly retards enzymatic digestion because of loss of flexibility in viral structure (breathing), which is required for protease activity. Indeed, the antiviral agent not only blocks digestion of internal residues but also protects the highly exposed NIm-IA antigenic site that lies ≈25 Å away from the bound drug (Figs. 1 and 3).

Furthermore, studies of naturally occurring HRV and polio mutants resistant to, and in some cases dependant on, WIN compounds show mutations not only in the drug-binding pocket but also distal to this site (16, 17). Our results substantiate the proposal that these distal mutations may impart drug resistance by decreasing the stability of the particles to compensate for WIN stabilization (16, 17). Finally, it has been shown that, whereas ICAM-1 (the cellular receptor recognized by the major group of rhinoviruses) binding to the southern portion of the canyon wall (9) destabilizes HRV14 (18), antibodies recognizing the NIm-IA site cause a stabilization effect. Antibodies recognizing other antigenic sites did not exhibit such stabilization effects (19). Because it is the NIm-IA site that is particularly sensitive to proteolytic cleavage in the absence of antiviral agents, results presented here suggest that antibody-mediated stabilization of virions may be caused by inhibition of conformational changes (breathing) around the NIm-IA site. The fact that the Fab portion (Fab17-IA) of a neutralizing antibody was observed to bind in the presence of
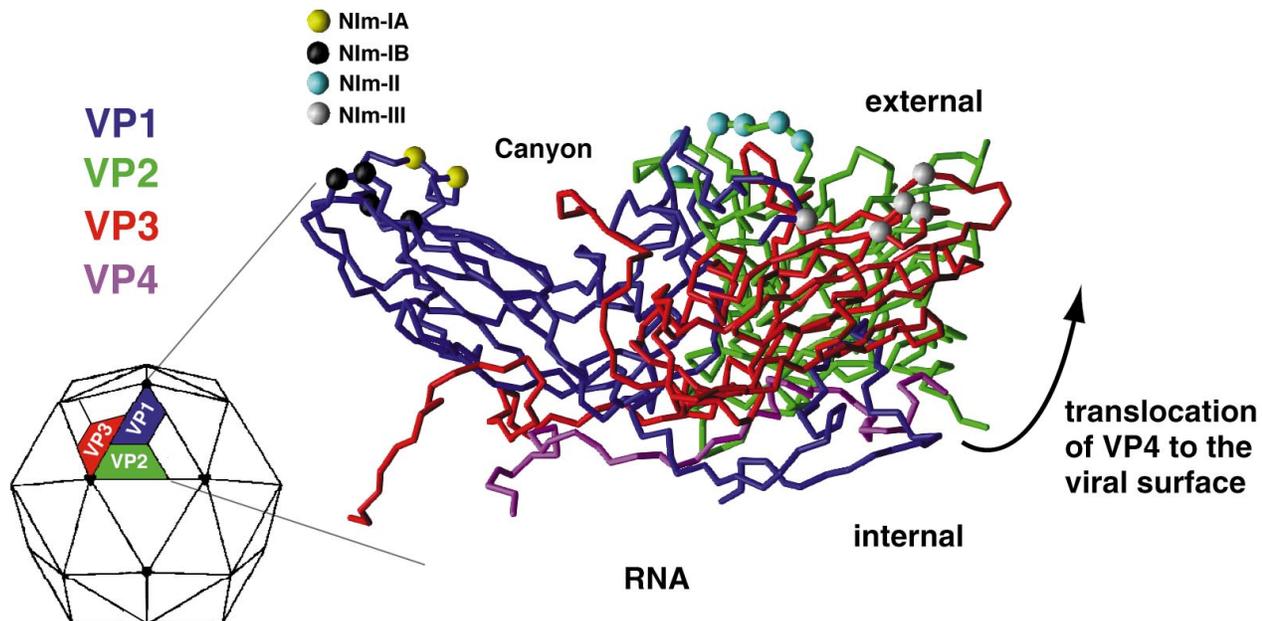

FIG. 2.   X-ray crystal structure of HRV14 shows VP4 to be the most internal viral protein. Time-course mass mapping of HRV14, however, reveals proteolytic fragments originating from VP4 within the first few minutes of viral digestion, demonstrating transient exposure of VP4 to the viral surface. The large arrow illustrates the translocation of VP4 from the interior of the capsid to the external viral surface (the arrow does not indicate the mechanism of the translocation). Also shown are the position of naturally occurring escape mutation sites for NIm-IA, NIm-IB, NIm-II, and NIm-III in yellow, black, cyan, and white, respectively.
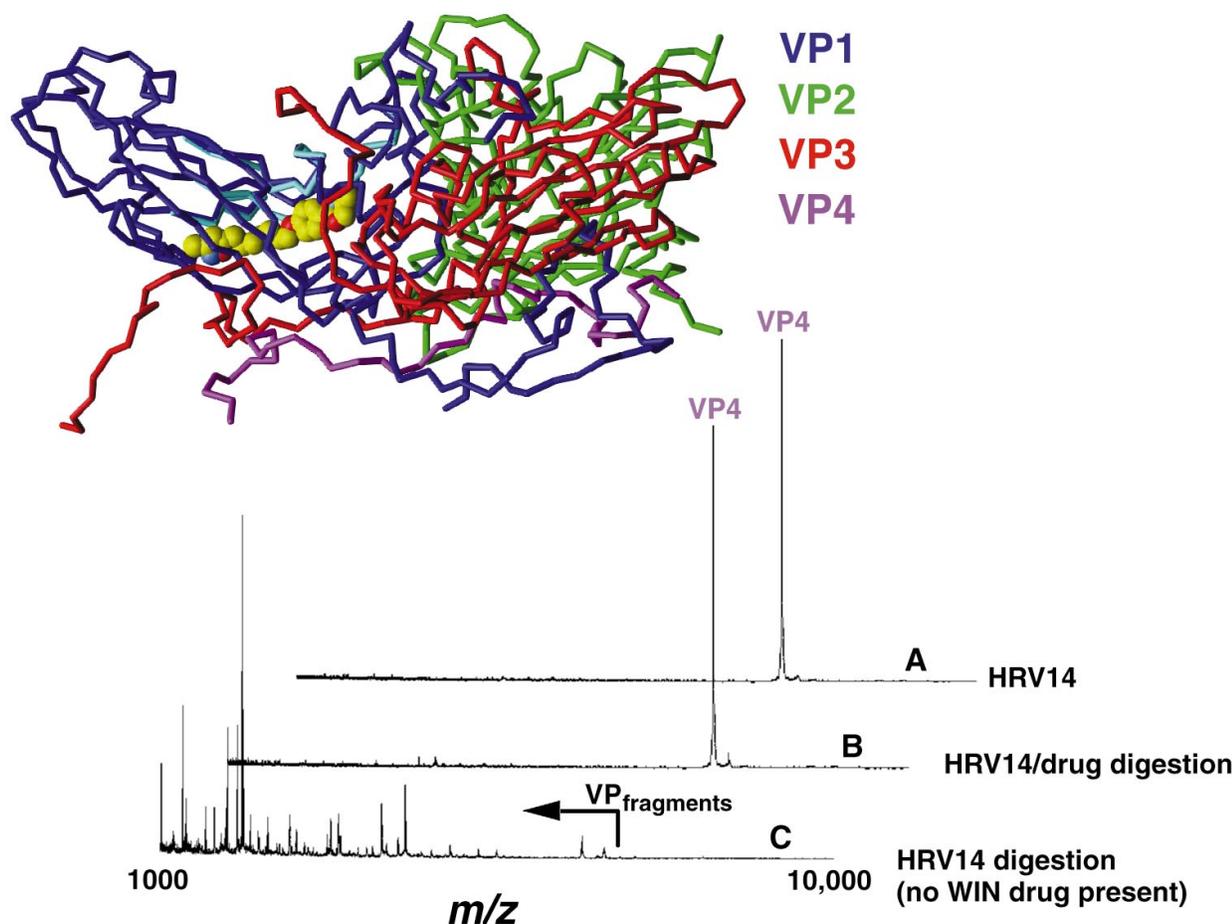
FIG. 3. HRV14 digestion with and without Win 52084 drug present. The MALDI-MS mass analysis was performed on HRV14 alone before digestion (*A*), after digestion of the HRV14/drug mixture (*B*), and after digestion of HRV14 alone (no drug present) (*C*). Digestions shown were performed for 3 h. It is important to note that in each case the virus was exposed for the same amount of time and the same concentration of enzyme; yet the drug-exposed virus was extremely resistant to digestion. Control experiments with FHV clearly demonstrated that the drug was not inhibiting the enzyme.

small hydrophobic compounds bound to the drug cavity (20) suggests that Fab17-IA is recognizing and stabilizing the structure represented by the atomic model. As proposed for
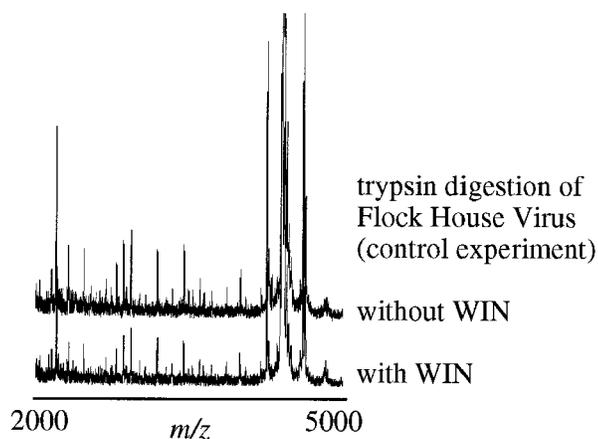

FIG. 4. Control experiment. Trypsin digestion of FHV (5) in the presence and absence of Win 52084. The off scale peak is the FHV γ-peptide (*m/z* 4,397 Da). Comparison of the resulting spectra shows the two sets of digestion fragments to be identical (within normal fluctuations of MALDI-MS signal intensity) and illustrates that inhibition of HRV14 digestion in the presence of the drug is a result of the HRV14-drug interaction and not Win 52084 inhibition of trypsin.

poliovirus (7, 15, 21), these results suggest that the canyon is a dynamic "trigger" region where a small amount of energy can result in large effects, either inducing or preventing uncoating. It is possible that WIN inhibits cellular attachment via this stabilization process rather than WIN-induced conformational changes, because not all of the major group rhinoviruses are affected to the same extent (22).

Interestingly, in our initial studies of HRV14 we observed the mass of VP4 to be 212 Da larger than predicted by the sequence (obtained from the Swiss-Prot Sequence Data Bank). Speculation as to the posttranslational modification of HRV14 structural proteins exists because of the observation of electron density, corresponding to the myristoylation of VP4 (23), in crystallographic data from HRV14. The 212-Da mass difference is consistent with VP4 myristoylation. Our results from further digestion and tandem MS structural studies of purified VP4 have localized myristoylation to the N terminus.

In conclusion, the observation of a highly dynamic capsid structure could fundamentally alter the way we look at viruses. Such observations, however, are not surprising given the events that shape the viral life cycle (1), a life cycle that demands a highly mobile viral surface. The use of MS (24) in combination with enzymatic probes (3–5) offers a unique means of examining dynamic events and also provides a complementary approach to the inherently static methods of crystallography and electron microscopy. The present results are consistent with those of previous studies (5, 7), which have also detected viral capsid mobility. Observation of drug-induced stability

clearly demonstrates the conformational restraint that the WIN drug provides. In addition and equally important, is the potential use of this method as a rapid and sensitive mass-based assay for studying antiviral-drug activity.

1. Rueckert, R. R. (1996) *Picornaviridae and Their Replication* (Raven, New York), pp. 609–654.
2. Rossmann, M. G., Smith, T. J. & Rueckert, R. R. (1993) *Structure Introductory Issue*, xxiv–xxv.
3. Cohen, S. L., Ferre-D'Amare, A. R., Burley, S. K. & Chait, B. T. (1995) *Protein Sci.* **4,** 1088–1099.
4. Kriwacki, R. W., Wu, J., Siuzdak, G. & Wright, P. E. (1996) *J. Am. Chem. Soc.* **118,** 5320–5321.
5. Bothner, B., Dong, X.-F., Bibbs, L., Johnson, J. E. & Siuzdak, G. (1998) *J. Biol. Chem.* **273,** 673–676.
6. Erickson, J. W., Frankenberger, E. A., Rossmann, M. G., Fout, G. S., Medappa, K. C., Rueckert, R. R. (1983) *Proc. Natl. Acad. Sci. USA* **80,** 931–934.
7. Li, Q., Yafal, A. G., Lee, Y. M. H., Hogle, J. & Chow, M. (1994) *J. Virol.* **68,** 3965–3970.
8. Rossmann, M. G., Arnold, E., Erickson, J. W., Frankenberger, E. A., Griffith, J. P., Hecht, H. J., Johnson, J. E., Kamer, G., Luo, M., Mosser, A. G., *et al.* (1985) *Nature* (*London*) **317,** 145–153.
9. Olson, N. H., Kolatkar, P. R., Oliveira, M. A., Cheng, R. H., Greve, J. M., McClelland, A., Baker, T. S. & Rossmann, M. G. (1993) *Proc. Natl. Acad. Sci. USA* **90,** 507–511.
10. Smith, T. J., Kremer, M. J., Luo, M., Vriend, G., Arnold, E., Kamer, G., Rossmann, M. G., McKinlay, M. A., Diana, G. O. & Otto, M. J. (1986) *Science* **233,** 1286–1293.
11. Pevear, D. C., Fancher, M. J., Felock, P. J., Rossmann, M. G., Miller, M. S., Diana, G., Tresurywala, A. M., McKinlay, M. A. & Dutko, F. J. (1989) *J. Virol.* **63,** 2002–2007.
12. Rombaut, B., Andries, K. & Boeye, A. (1991) *J. Gen. Virol.* **72,** 2153–2157.
13. Fox, M. P., Otto, M. J. & McKinlay, M. A. (1986) *Antimicrob. Agents Chemother.* **30,** 110–116.
14. Gruenberger, M., Pevear, D., Diana, G. D., Kuechler, E. & And, O. (1991) *J. Gen. Virol.* **72,** 431–433.
15. Hiremath, C. N., Filman, D. J., Grant, R. A. & Hogle, J. M. (1997) *Acta. Crystallogr.* D **53,** 558–570.
16. Mosser, A. G., Sgro, J. Y. & Rueckert, R. R. (1994) *J. Virol.* **68,** 8193–8201.
17. Mosser, A. G. & Rueckert, R. R. (1993) *J. Virol.* **67,** 1246–1254.
18. Hoover-Litty, H. & Greve, J. M. (1993) *J. Virol* **67,** 390–397.
19. Lee, W. M. (1992) Dissertation (University of Wisconsin, Madison).
20. Smith, T. J., Chase, E. S., Schmidt, T. J., Olson, N. H. & Baker, T. S. (1996) *Nature* (*London*) **383,** 350–354.
21. Chow, M., Basavappa, R. & Hogle, J. (1997) in *Structural Biology of Viruses,* eds. Chiu, W., Burnett, R. M. & Garcea, R. L. (Oxford, New York), pp. 157–186.
22. Pevear, D. C., Diana, G. D. & McKinlay, M. A. (1992) *Semin. Virol.* **2,** 41–55.
23. Arnold, E. & Rossmann, M. G. (1990) *J. Mol. Biol.* **211,** 763–801.
24. Siuzdak, G. (1996) *Mass Spectrometry for Biotechnology* (Academic, San Diego, CA).
25. Smith, T. J. (1995) *J. Mol. Graphics* **13,** 122–125.